



Behaviour of LSF Floor Systems with Improved Joist Sections under Fire Conditions

V. Jatheeshan¹, M. Mahendran²

Abstract

Fire safety design of buildings is essential to safeguard lives and minimize the loss of damage to properties. Light-weight cold-formed steel channel sections along with fire resistive plasterboards are used to construct light gauge steel frame floor systems to provide the required fire resistance rating. However, simply adding more plasterboard layers is not an efficient method to increase FRR. Hence this research focuses on using joists with improved joist section profiles such as hollow flange sections to increase the structural capacity of floor systems under fire conditions and thus their FRR. In this research, the structural and thermal behaviour of LSF floor systems made of LiteSteel Beams with different plasterboard and insulation configurations was investigated using four full scale tests under standard fires. Based on the ultimate failure load of the floor joist at ambient temperature, transient state fire tests were conducted for different Load Ratios. These fire tests showed that the new LSF floor system has improved the FRR well above that of those made of lipped channel sections. The joist failure was predominantly due to local buckling of LSB compression flanges near mid-span with severe yielding of tension flanges. Fire tests have provided valuable structural and thermal performance data of tested floor systems that included time-temperature profiles, and failure times and temperatures. Average failure temperatures of LSB joists and reduced yield strengths were used to predict their ultimate moment capacities, which were compared with corresponding test capacities. This allowed an assessment in relation to the accuracy of current design rules for steel joists at elevated temperatures. This paper presents the details of full scale fire tests of LSF floor systems made of LSB joists with different plasterboard and insulation configurations and their results along with some important findings.

1. Introduction

Cold-formed steel channels are the prominent sections used as floor joists in light-weight steel building industry. In these applications of Light gauge Steel Frame (LSF) floor systems, thin-walled cold-formed steel sections are protected by multiple plasterboard layers to provide the required Fire Resistance Rating (FRR). In common practice, lipped channel sections are used as floor joists in the construction of LSF floor systems. But open and thin lipped channel sections are not often structurally capable under fire conditions. Other section profiles can also be used as

¹PhD Researcher, Queensland University of Technology <jatheeshan.varathananthan@student.qut.edu.au>

² Professor, Queensland University of Technology, <m.mahendran@qut.edu.au>

joists and among them LiteSteel Beam (LSB) sections with rectangular hollow flanges are structurally more efficient for which the occurrence of local and distortional buckling are eliminated to an extent, when they are used as joists in LSF floor systems. Anapayan et al. (2011) have shown that these LSB sections have high bending capacities at ambient temperatures. These sections may also be structurally efficient during fire conditions. During fire events floor joists are exposed to non-uniform temperature distribution across the joist. Therefore their behaviour is quite different to ambient temperature conditions. Previous researchers such as Sultan et al. (1998), Alfawakhiri (2001), Sakumoto et al. (2003), Kaitila (2002), Zhao et al. (2005) and Baleshan and Mahendran (2010) have conducted research on LSF floor systems made of lipped channel sections under fire conditions. However, the behaviour of LSF floors made of improved joist sections such as LSBs has not been investigated under fire conditions. Therefore this research was conducted to investigate the structural and thermal behaviour of LSF floor systems made of LSBs under fire conditions and to predict their FRR. It was also investigated the effects of the number of plasterboard layers, cavity insulation and load ratio by considering different floor configurations.

Generally in floor systems, fire initiates and spreads upwards towards the ceiling side of the floor systems. Therefore the ceiling side needs to be protected using fire resistive boards. Fire resistive gypsum plasterboards are used below the floor frame as the barrier to provide the required fire resistance to the floor systems. Plywood is generally used as the subfloor to provide the required structural resistance even at elevated temperatures. Since full scale fire tests were conducted under laboratory conditions in this research, plasterboards were used to simulate the subfloor to avoid burning of plywood. During later stages of tests, unexposed side plasterboards start to bend under load, weakening their connectivity to the joists and therefore the lateral restraints usually available to the floor joists' compression flanges will not be available. This paper presents the details of the full scale fire tests and their results and also the comparisons of test results with predictions based on available fire design rules in cold-formed steel design standards.

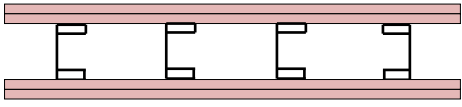
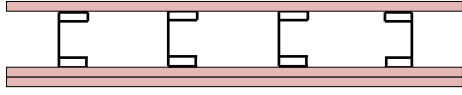
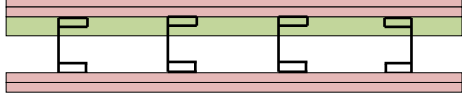
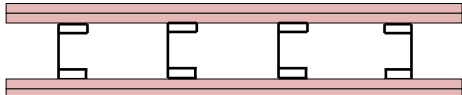
2. Full Scale Fire Tests of LSF Floor Systems

2.1 Test Specimens

Four full scale tests were conducted to study the structural and thermal behaviour of LSF floor systems made of LSBs under standard fires (Table 1). Test Specimens 1 and 4 were similar in terms of the floor configurations but these tests were conducted for a Load Ratio (LR) of 0.2 and 0.4, respectively. Test Specimens 1 and 4 consisted of two layers of plasterboards on both sides while Test Specimen 2 consisted of a single layer of plasterboard. Test Specimen 3 consisted of two layers of plasterboards on both sides with rock fibre insulation inside the floor cavity.

In all the tests, floor frame was fabricated using four 200 x 45 x 15 x 1.6 mm LSB joists at 600 mm spacing and connected with two tracks on top and bottom using D-type flat head 25 mm long 10 gauge screws. It was protected against direct fire exposure by using fire resistive Type-X gypsum plasterboards. The 2400 mm x 1200 mm plasterboards supplied were 16 mm in thickness with a density of 13 kg/m² and were manufactured to the requirements of AS/NZS 2588 (SA 1998) and fixed according to AS/NZS 2589.1 (SA 1997).

Table 1: Details of full scale fire tests

Test	Floor Configuration	Insulation	Load Ratio
1		-	0.2 (15.4kN per joist)
2		-	0.2 (15.4 kN per joist)
3		Rock fibre	0.2 (15.4 kN per joist)
4		-	0.4 (30.8 kN per joist)

Fire Side (FS) base layer was attached to the floor frame using two 2100 mm x 1200 mm plasterboards as they create a horizontal plasterboard joint across the joists using D-type 50 mm long screws as shown in Fig. 2 (a). The screws were fastened at 200 mm intervals and a minimum edge distance of 10 mm was maintained for all the plasterboard joints. The FS face layer plasterboard was then attached on top of the base layer in the same manner using one 2100 mm x 1200 mm, one 2100 mm x 1000 mm and one 2100 mm x 200 mm plasterboards as they create two horizontal joints and also staggering the base layer plasterboard joint by 200 mm. The plasterboard joints were sealed using 50 mm wide cellulose based joint tape sandwiched between two coats of joint filler paste. 150 x 45 x 15 mm channel sections were fixed at every 600 mm to provide the required lateral restraints to the floor joists as shown in Fig. 2 (b). In Test Specimen 3, three layers of 25 mm thick rock fibre insulation were attached within the cavity using S-type 100 mm long bugle head screws and 50 mm diameter guard head washers as shown in Fig. 2 (b).

K-type thermocouples with a limit of 1200°C were used to measure the temperatures on the steel and plasterboard surfaces along and across the floor specimen. They were attached to the Outer Hot Flange (OHF), Inner Hot Flange (IHF), middle web, Inner Cold Flange (ICF) and Outer Cold Flange (OCF) surfaces of the joist section at quarter-length (0.25h), half-length (0.5h) and three quarter-length (0.75h) of the joists. Thermocouples were also attached on Fire Side (FS), FS face layer (Pb1)-FS base layer (Pb2), Pb2-Cavity, Cavity-Ambient side base layer (Pb3), Pb3-Ambient side face layer (Pb4) and Ambient Side (AS) surfaces at quarter-lengths (0.25h, 0.5h and 0.75h). Fig. 1 shows the thermocouple locations across the floor specimen.

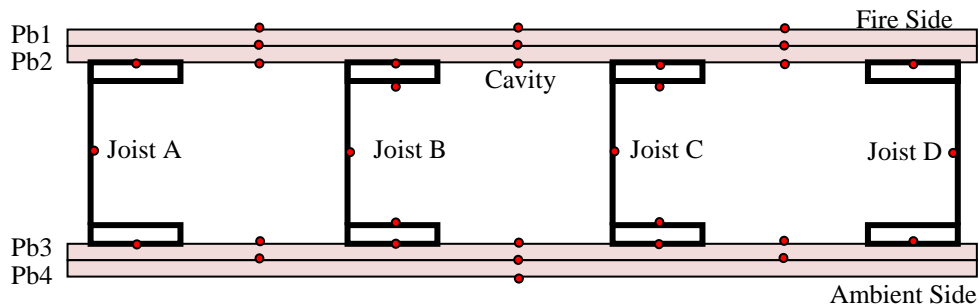
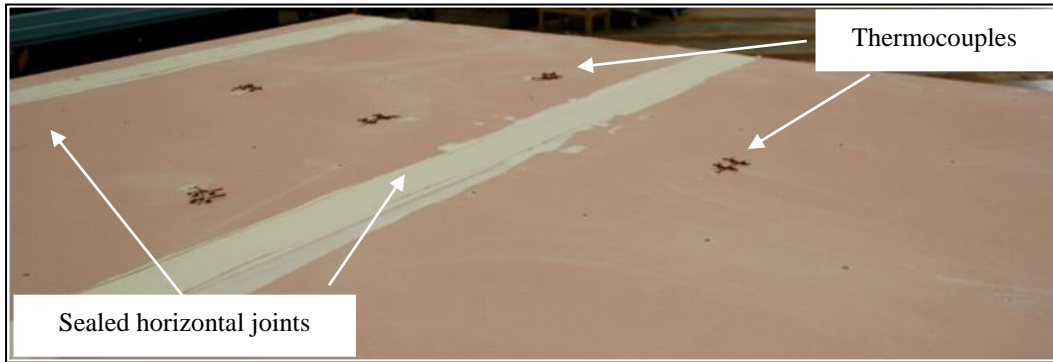


Figure 1: Locations of thermocouples on LSF floors



(a) Fire side base layer



(b) LSF floor specimen

Figure 2: Floor specimen

2.2 Test Set-up

A propane gas furnace designed and built in accordance with AS 1530.4 (SA 2005) was used to conduct the fire tests. The furnace temperature was measured using four 600 mm long Nicrobell coated rod type thermocouples and the average temperature rise of these thermocouples was provided as the input to the control system of the furnace based on the standard cellulosic time-temperature fire curve given in AS 1530.4 (SA 2005). A heavy H-frame was specially constructed and two heavy angle sections were welded on top and bottom side of the H-frame to simply support the floor system as shown in Fig. 3. The gas furnace allows the floor specimen to be tested only in the vertical direction. Therefore the floor specimen was mounted within the H-frame and the load was applied from one side using a horizontal load distribution system.

In order to simulate a uniformly distributed load, a load distribution system was developed to apply quarter length point loads to the joists. Two 100 kN hydraulic jacks were connected to the loading system and the load was monitored using two 100 kN load cells and the other ends of the jacks were placed on jack holders which were connected to the two vertical columns in front of the floor specimen as shown in Fig. 3. Deflections of the floor specimen were measured using 10 LVDTs located at quarter, half and three quarter lengths of the floor specimen.

2.3 Test Procedure

Initially the floor specimen was mounted within the heavy H-frame and was simply supported against the two heavy angle sections located at the top and bottom using G-clamps. The loading

set-up was then fixed by connecting it to the end plates attached to the floor specimen. A hydraulic pump was used to apply and control the load. The furnace was moved towards the floor specimen to fill any gap between them. Following this, the floor specimen was exposed to fire from one side and structural load from the other side. Finally all the thermocouples, LVDTs and load cell cables were connected to the UDAQ system for measurements during the tests.

Load Ratio (LR) is the ratio of the load used in the fire test and the load at ambient temperature conditions. Tests 1 to 3 were conducted under a LR of 0.2 while Test 4 was conducted under a LR of 0.4. Initially the ambient temperature ultimate failure load of 1.6 mm thick 200 mm x 45mm x 15 mm LSB joist section was predicted using numerical modelling and was validated using AS/NZS 4600 (SA 2005) design rules. The ultimate failure load determined using the design rules was 77.1 kN. Therefore the load applied in Tests 1 to 3 was 15.4 kN per joist while it was 30.8 kN per joist in Test 4. The applied load was maintained when the floor specimen was exposed to the standard time-temperature profile (Fig. 4). The applied load, lateral deflection and temperature measurements were recorded at every 10 seconds. Test specimen was considered to have failed when the oil pressure in the jacks could not be maintained (Fig. 5). Test was stopped immediately following the failure of the floor specimen and the time to failure was recorded.

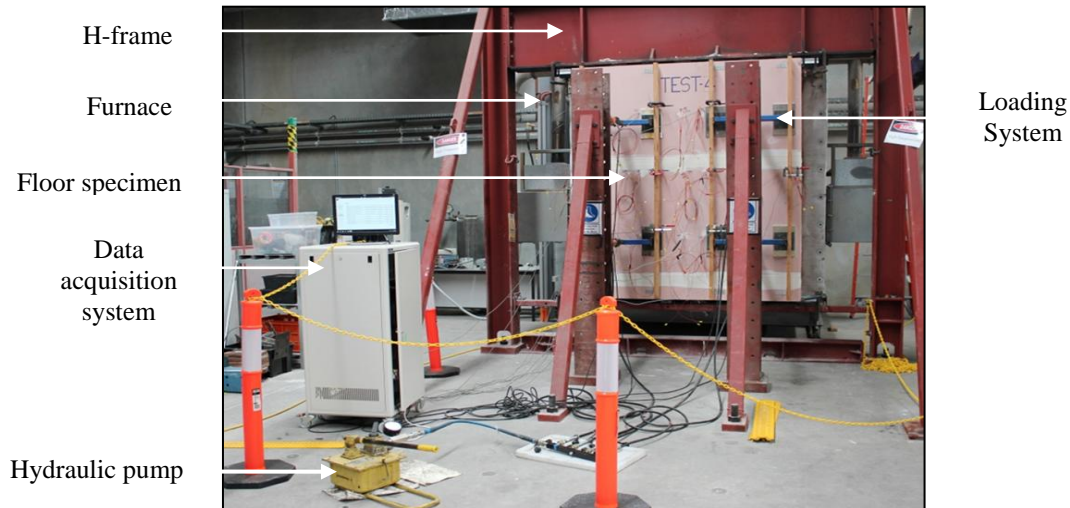


Figure 3: Overall test set-up

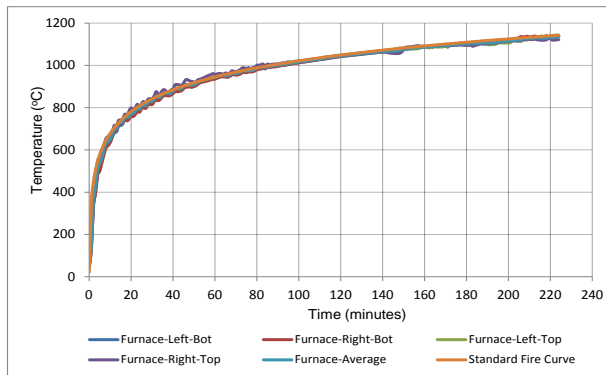


Figure 4: Furnace temperature and standard fire curve

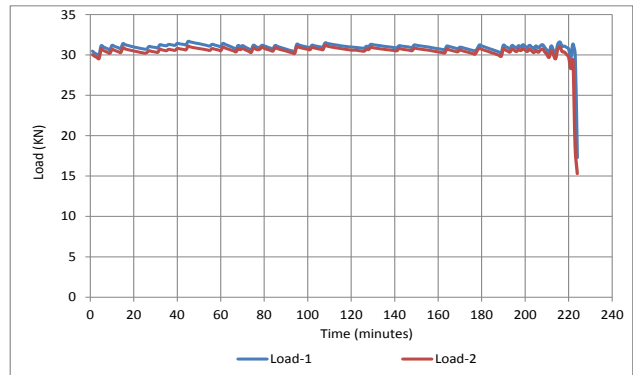


Figure 5: Applied load variation with time

3. Observations and Results

3.1 Visual Observations

In all four tests, smoke started to escape through the top left side of the specimen after a few minutes due to the burning of the paper of the exposed plasterboard. The smoke intensity eventually decreased. This process was repeated when each plasterboard surface paper was burnt. In addition to the smoke, water drops were observed on the H-frame and the bottom RHS due to the evaporation of free and chemically combined water in the gypsum plasterboards. In addition, the floor specimen was observed to laterally deflect towards the furnace in all four tests. This lateral deflection was higher in the interior joists (Joists B and C) than in the exterior joists (Joists A and D). This lateral deflection caused bending of the ambient side plasterboards and a curves shape crack due to the low bending capacity of gypsum plasterboard.

Fig. 6 (b) shows that the face and base layers of the fire side plasterboards had fallen off at mid-span and Joists B and C were directly exposed to fire for some time. At the remaining places only the face layer had fallen off and the base layer was intact with steel joists. The failure of Joists B and C occurred predominantly due to local buckling of the compression (cold) flanges with severe yielding of tension (hot) flanges. In Test 2, the failure occurred earlier than Test 1 due to the usage of only a single layer of plasterboard and the failure mode of the floor joist was similar to Test 1. Fig. 8 shows the failed floor specimens of Tests 1 and 3. Fig. 9 shows the local buckling failures of the individual joists from all three tests. In Test 3, the failure of the floor specimen occurred after a larger lateral deflection compared to Tests 1 and 2 due to the presence of cavity insulation. Cavity insulation caused a higher temperature difference across the joists and thus higher thermal bowing and lateral deflections as shown in Fig. 7 (b). Test 4 was terminated prematurely after 150 minutes due to the dislocation of screw connections of Joist B and track at the support. This was caused by the the higher load in Test 4 and the associated larger deflections in the floor specimen.



(a) Lateral deflection of floor specimen



(b) Partial fall-off of fire side plasterboards

Figure 6: Floor specimen after failure in Test 1

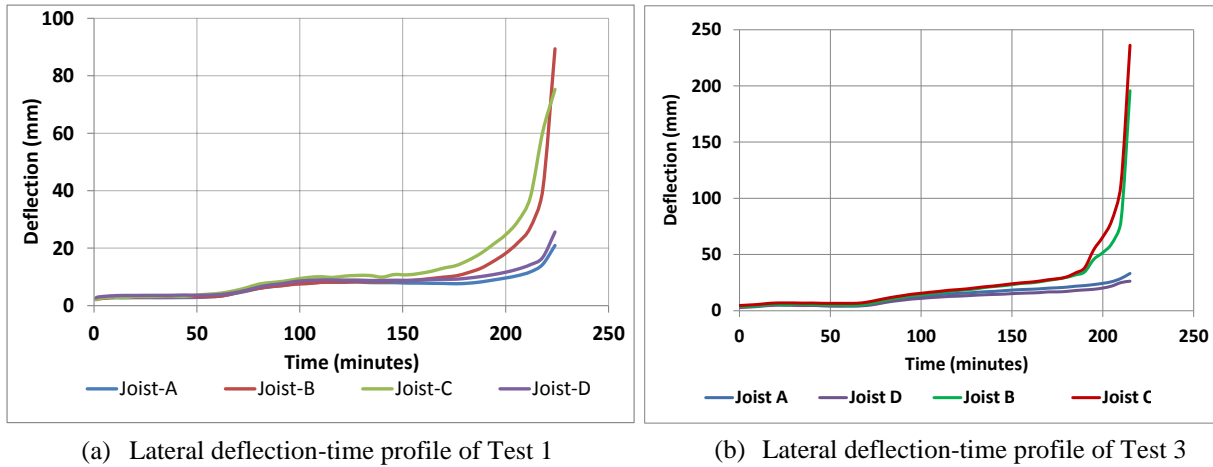


Figure 7: Lateral deflection versus time curves

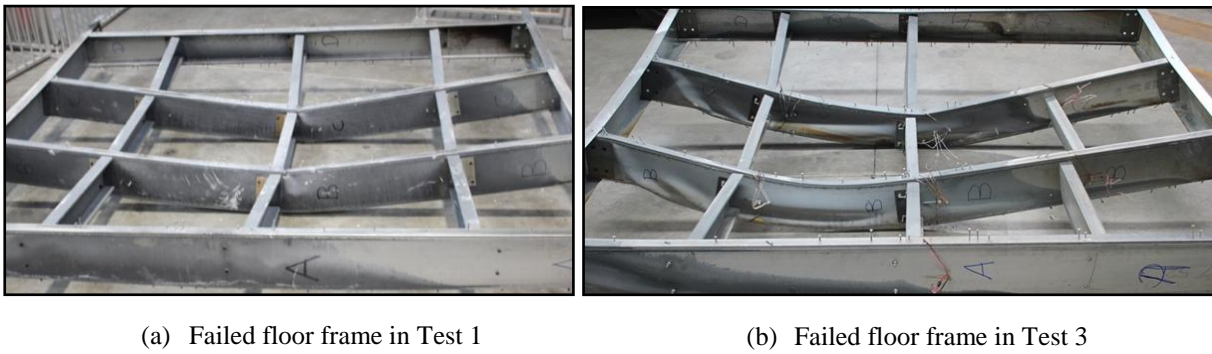


Figure 8: Tested floor frames after failure

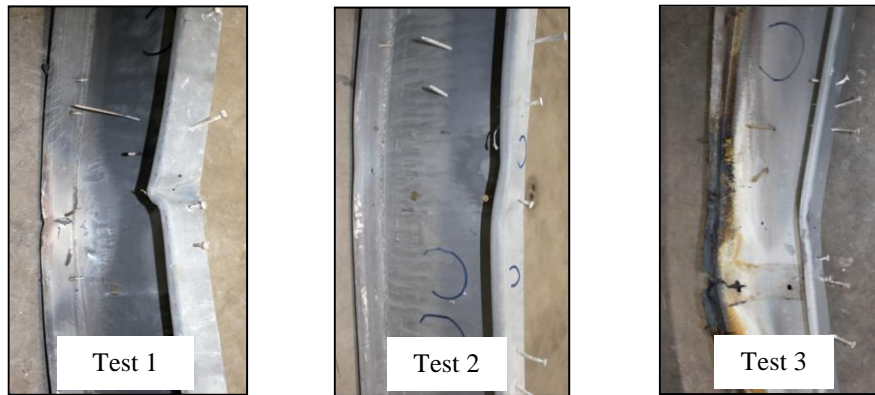


Figure 9: Local buckling failure of joists in Tests 1 to 3

3.2 Results

Full scale fire tests have provided important results including time-temperature profiles of plasterboard and steel joist surfaces, and failure times and failure modes for different floor panel configurations. These results include the average outer hot flange, web and outer cold flange failure temperatures of floor joists for different floor panel configurations and load ratios. Table 2 provides the details of LSF floor fire tests and the important results from each test.

3.2.1 Test 1

In Test 1, the failure of floor specimen occurred at 222 minutes. Figs. 10 and 11 show the average time-temperature profiles of plasterboard and steel joist surfaces, respectively. In Fig. 10 the time-temperature profile of Pb1-Pb2 consists of three different phases. After 2 minutes from the start of the test, the temperature increased to 85°C in 3 minutes. For the next 17 minutes, the temperature increased slowly and steadily until 120°C, during which the dehydration process occurred when steam and water particles were observed. Following this the temperature increased from 120°C to 630°C by 80 minutes. From 80 minutes, the rate of temperature rise was reduced with time due to the dehydration of the next plasterboard and reached 820°C by 155 minutes. Thereafter the average time-temperature profile of Pb1-Pb2 increased suddenly and reached the temperature of FS plasterboard surface due to the fall-off of the plasterboard pieces.

The average time-temperature profiles of Joist B are shown in Fig. 11, which also shows three different phases. The time-temperature profiles show a clear reduction in temperature from hot to cold side. Firstly, Outer Hot Flange (OHF) shows the highest temperature development, followed by Inner Hot Flange (IHF), web, Inner Cold Flange (ICF), and finally Outer Cold Flange (OCF) shows the lowest. After 158 minutes, the temperature increased rapidly in OHF and IHF surfaces of Joist B. Web, ICF and OCF also followed the same pattern as the OHF. This rapid rise in temperature relates to the observed plasterboard fall-off after 158 minutes.

Table 2: Results of LSF floor tests

Details	Test 1	Test 2	Test 3
LSF floor panel configurations	Dual plasterboards on both sides	Single plasterboard on both sides	Dual plasterboards on both sides
Insulation	None	None	Cavity insulation- Rock fibre
Load ratio	0.2	0.2	0.2
Failure time (minutes)	222	163	214
Failure type	Local buckling of compression flanges with severe yielding of tension flanges	Local buckling of compression flanges with yielding of tension flanges	Local buckling of compression flanges with severe yielding of tension flanges
Maximum lateral deflection (mm)	90	89	236
Avg. failure joist temperatures			
▪ Outer Hot Flange (°C)	712	715	901
▪ Middle Web (°C)	666	636	685
▪ Outer Cold Flange (°C)	601	595	573

3.2.2 Test 2

In Test 2, the failure occurred at 163 minutes due to the use of a single plasterboard layer on fire side. Figs. 12 (a) and (b) show the average time-temperature profiles of plasterboard and steel surfaces, respectively. Plasterboards have three stages of temperature development as in Test 1. Fig. 12 (b) shows that the temperature development was consistent in Joists B and C. After 110 minutes, the average OHF, web and OCF temperature profiles showed a rapid rise in both joists since the temperature at mid-height had increased due to the weakened plasterboard joint.

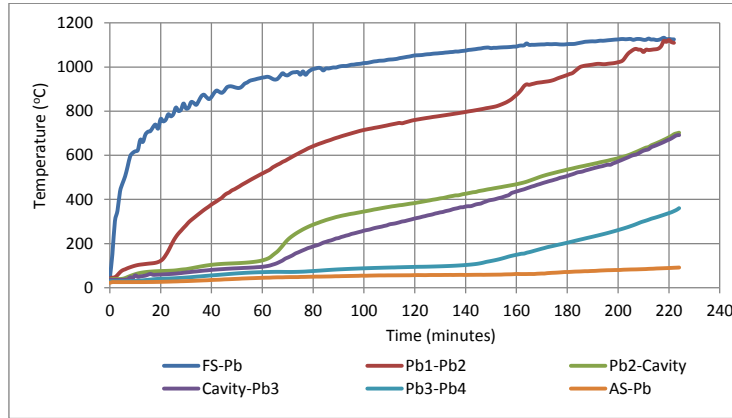


Figure 10: Average time-temperature profiles of plasterboard surfaces in Test 1

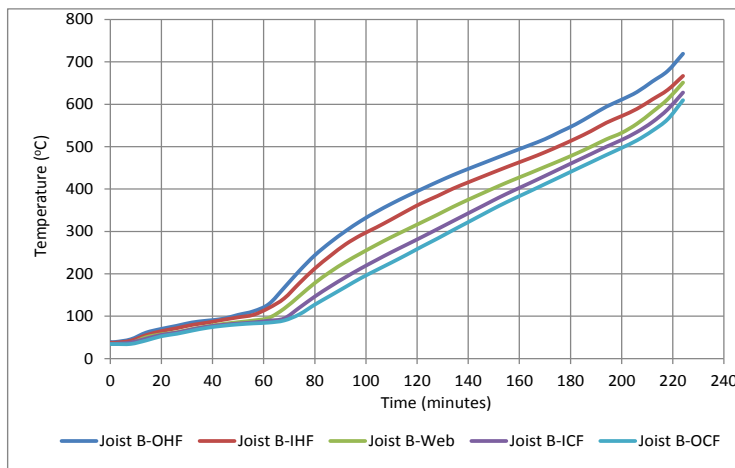
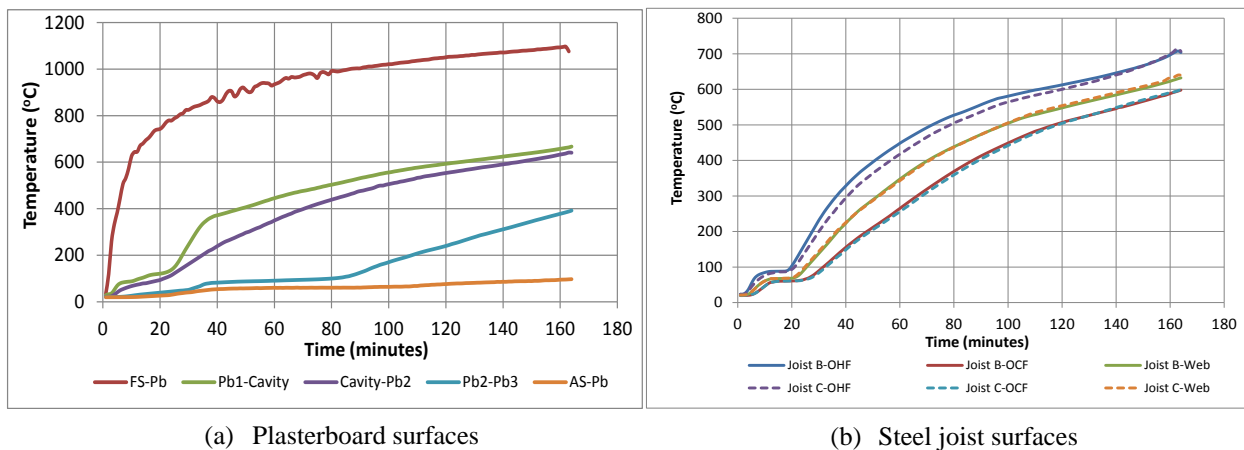


Figure 11: Average time-temperature profiles of steel joist surfaces in Test 1



(a) Plasterboard surfaces

(b) Steel joist surfaces

Figure 12: Average time-temperature profiles of plasterboard and steel joist surfaces in Test 2

3.2.3 Test 3

The failure occurred at 214 minutes with a larger deflection than in previous tests. The face and base layers of fire side plasterboards had fallen off at the middle level and Joists B and C were directly exposed to fire for some time. Joists B and C had the maximum deflections of 195 mm

and 236 mm, respectively, at mid-height. This was due to the observed higher thermal bowing effect caused by the higher temperature difference across the middle joists. Fig. 13 shows the average time-temperature profiles of plasterboard and steel surfaces. It can be seen that the OHF time-temperature profiles are much higher than others due to the presence of cavity insulation.

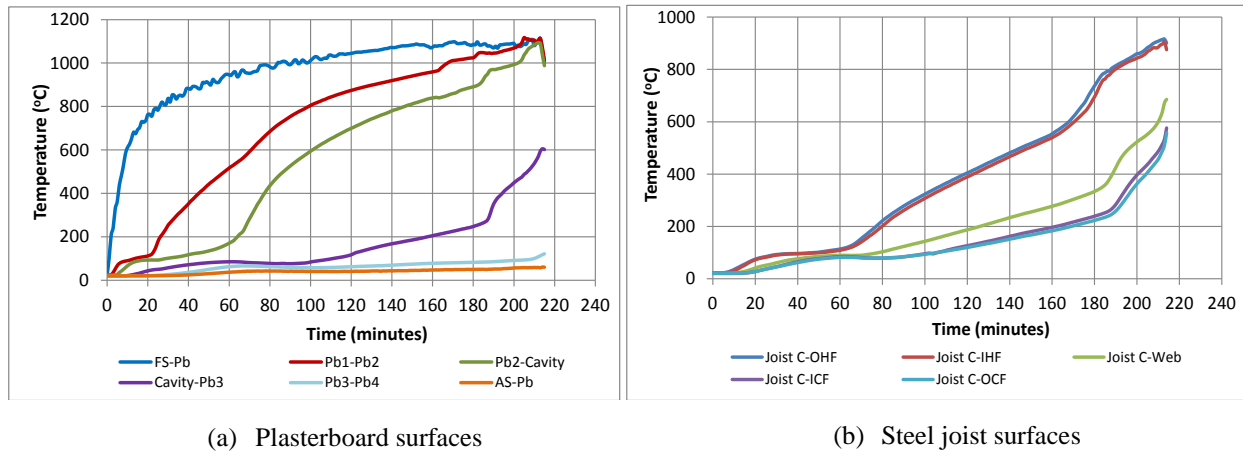


Figure 13: Average time-temperature profiles of plasterboard and steel surfaces in Test 3

4. Discussions

This section discusses the differences in failure times and temperatures for Tests 1 to 4. The comparisons between the test results are based on the effect of load ratio, influence of cavity insulation, number of fire side plasterboards, effect of plasterboard joints and influence of plasterboard fall-off. In addition, the performances of LSF floors made of LSBs and conventional lipped channel sections are also compared and discussed.

4.1 Effect of load ratio

Effects of load ratio on the behaviour of LSF floor systems are investigated by comparing the results of Tests 1 and 4 conducted for load ratios of 0.2 and 0.4, respectively. The average time-temperature profiles of plasterboard surfaces across the specimen (FS, Pb1-Pb2, Pb2-Cavity, Cavity-Pb3, Pb3-Pb4 and AS) are compared in Fig. 14 (a) while Fig. 14 (b) compares the steel joist surface profiles. These time-temperature profiles agree quite well. In Test 1 due to the plasterboard fall-off, the temperature profile of Pb1-Pb2 suddenly increased, but in Test 4 plasterboard fall-off did not occur until it was terminated. This comparison clearly shows that the load ratio does not have any effect on the temperature development of steel joist surfaces.

4.2 Effect of horizontal plasterboard joint

The floor panel was constructed using two 2400 mm x 1200 mm plasterboards with a horizontal joint in the middle. The joint was sealed using a sealant with a joint tape sandwiched between two coats of joint sealant as shown in Fig. 15. During fires this plasterboard joint plays a major role in the development of temperature on steel surfaces. The plasterboard joint is the weakest part and therefore during fire it may crack due to high temperatures and larger lateral deflection can occur at mid-span. This allows the heat to penetrate through the gap formed by the crack. Fig. 16 shows the comparison of OHF time-temperature profiles of steel joists along the length in Test 2 with single plasterboard lining. A difference in the temperature development can be seen after about 110 minutes at mid-level due to the weakening of the horizontal plasterboard joint.

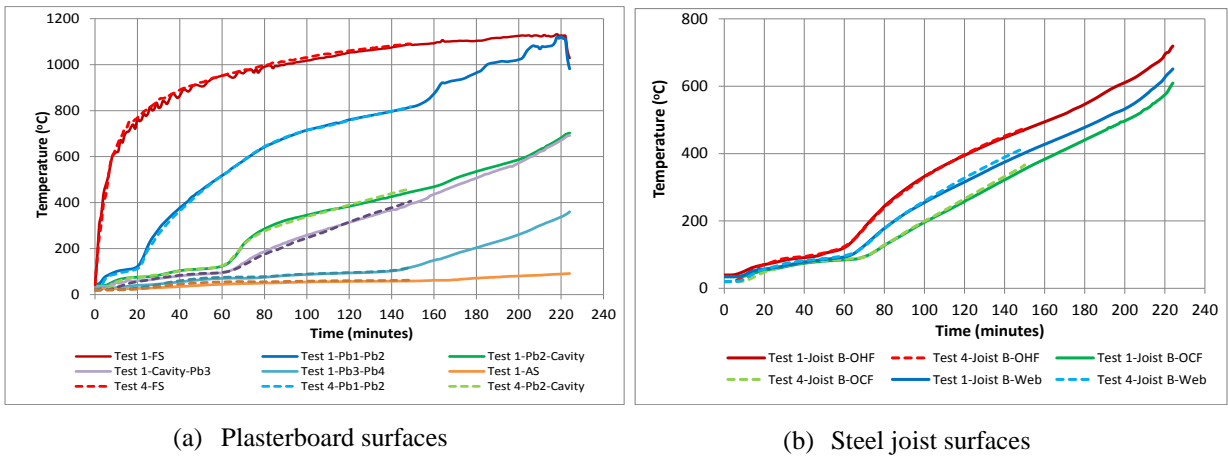


Figure 14: Average time-temperature profiles of plasterboard and steel surfaces in Tests 1 and 4

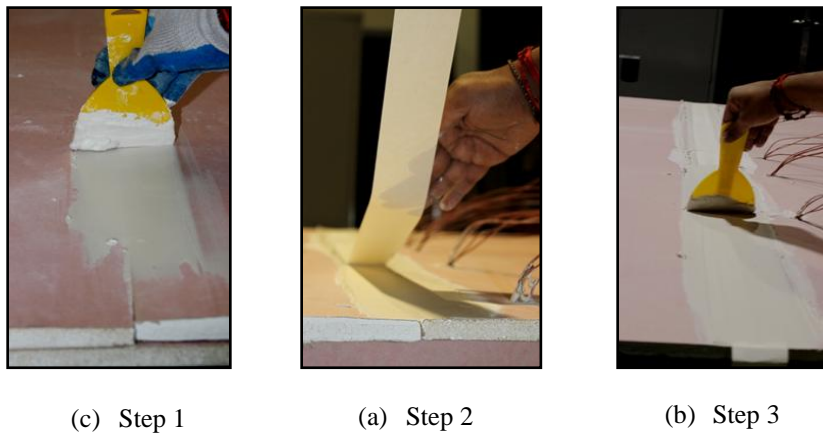


Figure 15: Plasterboard joint sealing process

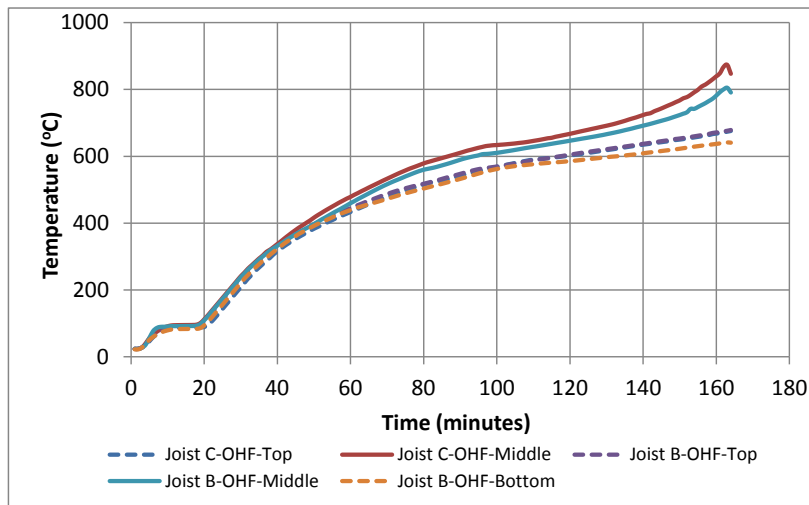


Figure 16: OHF time-temperature profiles of middle joists in Test 2

4.3 Influence of plasterboard fall-off

The fire side plasterboard layers protect the steel joists from rapid temperature rise. During fire, Pb1 softens after the calcination process and falls-off. Hereafter, the temperature of Pb1-Pb2 will become equal to FS temperature within a short period and the temperature development in steel joists will be rapid. Fig. 17 shows the time-temperature profiles of plasterboard surfaces in Tests 1 and 3. In Test 1, after about 160 minutes the temperatures of Pb1-Pb2 at different locations start to increase rapidly due to the fall-off of Pb1. The fall-off of plasterboard initiated at mid-height at a temperature of 850°C and then continued to top and bottom heights. At the time of failure, Pb1 had fallen-off in almost all the places and by then Pb1-Pb2 temperature had reached 1100°C. In Test 3, in addition to the fall-off of Pb1, Pb2 had also started to fall-off after about 180 minutes. The FS, Pb1-Pb2 and Pb2-Cavity surfaces had almost the same temperature at failure. This had a huge impact on the temperature development of steel joist surfaces in Tests 1 and 3 after 160 minutes as shown in Fig. 18 (b), which clearly shows that steel temperatures have risen rapidly in both tests after the fall-off of plasterboards.

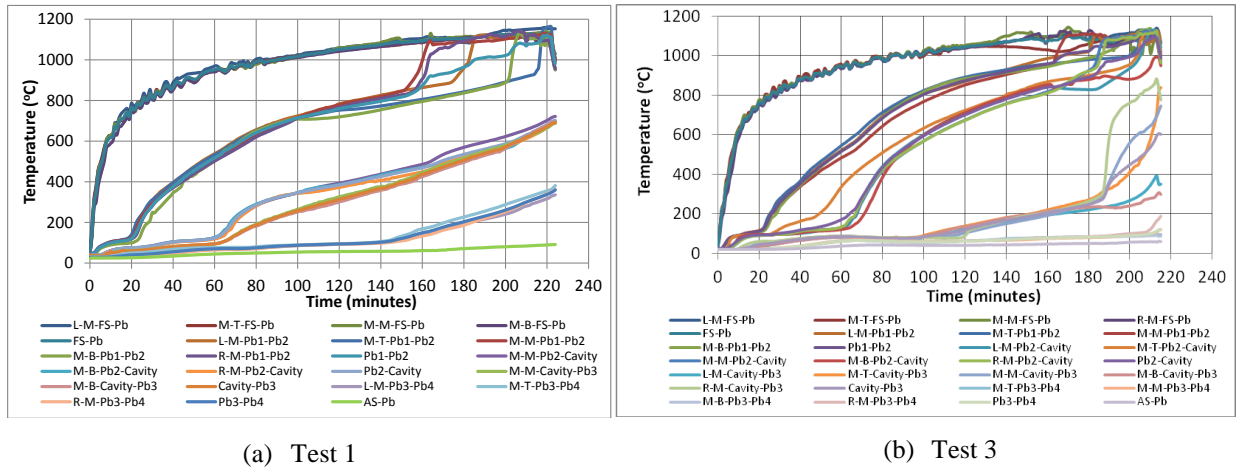
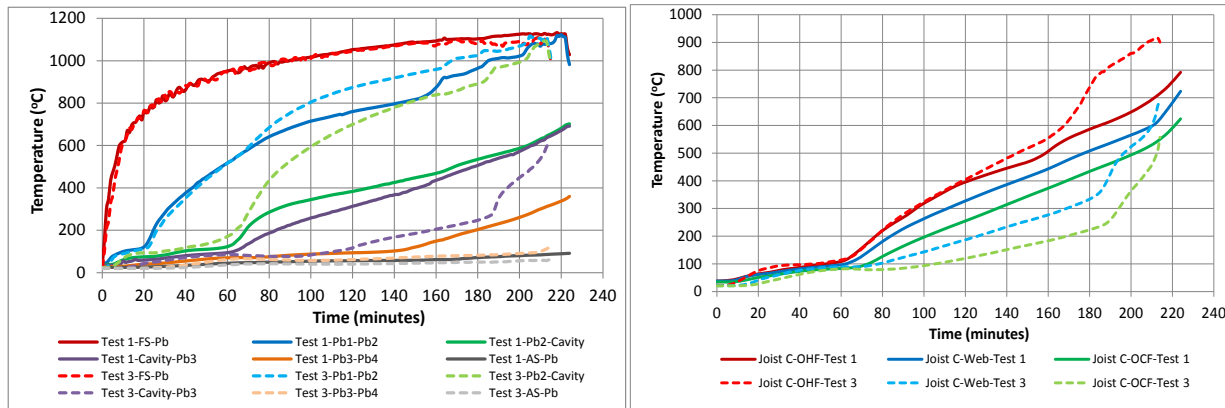


Figure 17: Time-temperature profiles of plasterboard surfaces at individual locations

4.4 Effect of cavity insulation

Figs. 18 (a) and (b) show the time-temperature profiles of plasterboard and steel surfaces from Tests 1 and 3, respectively. FS temperatures of Tests 1 and 3 are similar and Pb1-Pb2 temperature is also the same until 70 minutes. After the dehydration process of Pb1 (70 minutes), the heat transfer through floor cavity was resisted by cavity insulation. Therefore in Test 3 the temperature rise in Cavity-Pb3 and Pb3-Pb4 surfaces were lower than that in Test 1 while the temperatures of Pb1-Pb2 and Pb2-Cavity surfaces increased at a higher rate in Test 3 than in Test 1. Also the OHF surface temperatures in Test 3 were seen to rise rapidly after 120 minutes with large temperature differences across the joist sections due to the prevention of heat transfer to ambient side by the cavity insulation. The temperatures of web and OCF in Test 3 were lower than in Test 1 from 70 minutes with a steady increase in the difference. After 180 minutes, OHF, web and OCF temperatures increased rapidly in Test 3 due to the fall-off of Pb2 unlike in Test 1. At failure the OHF temperature difference between Joists C in Tests 1 and 3 reached around 150°C. The difference between the failure times is due to this higher temperature difference across the joist in Test 3 and associated larger thermal bowing and lateral deflections. However, the failure modes in both Tests 1 and 3 were the same, i.e. Compression flange local buckling with severe yielding in tension flanges of interior joists.



(a) Plasterboards surfaces

(b) Steel joist surfaces

Figure 18: Comparison of average time-temperature profiles from Tests 1 and 3

4.5 Effect of using LSB joist section

Test conditions of the full scale fire tests conducted by Baleshan and Mahendran (2010) are similar to the current study. They used lipped channel section floor joists. In this section, the results of Tests 1 and 3 are compared with their results (Tests B1 and B2).

Table 3 summarizes the details and results of these full scale fire tests. In the current study, all the test specimens were constructed using dual plasterboards on the ambient side to simulate the subfloor. Baleshan and Mahendran (2010) used plywood on the ambient side to simulate the subfloor conditions in Test B1. But in Test B2, dual plasterboards were used on the ambient side to avoid burning of plywood. In Tests 1 and 3 the joist failure was predominantly due to local buckling of cold compression flanges with severe yielding of hot tension flanges at mid-span. In this study, 6 mm web plates were used to strengthen the thinner web elements of the floor joists near the support. But in Tests B1 and B2, the failures occurred due to local web buckling near the support. This is possibly due to not using web plates to strengthen the joists with thin webs.

Table 3: Comparison of fire test results from this study and Baleshan and Mahendran (2010)

Tests	Load Ratio	Failure type	Failure time (minutes)	Failure joist temperature (°C)	
				Outer Hot Flange	Outer Cold Flange
Test 1	0.2	Local buckling of compression flanges with severe tension flange yielding at mid-span	222	712	601
Test 3	0.2	Local buckling of compression flanges with severe tension flange yielding at mid-span	214	901	573
Test B1	0.4	Local buckling of web at the support	107	489	346
Test B2	0.4	Local buckling of web at the support	99	504	106

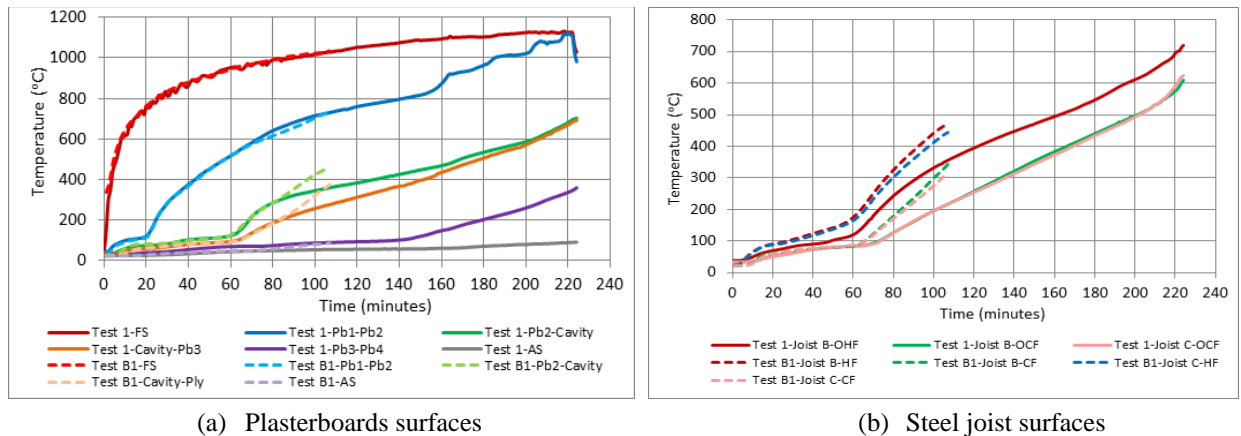


Figure 19: Average time-temperature profiles compared in between Tests 1 and B1

Figs. 19 (a) and (b) compare the average time-temperature profiles of plasterboard and steel surfaces between Tests 1 and B1. Fig. 20 (a) and (b) compare them for Tests 3 and B2. In Figs. 19 and 20 (a), the FS and Pb1-Pb2 surface temperatures of both tests have shown a good agreement. In Fig. 19 (b), initially there is a difference of 40°C in the hot flange temperatures until 80 minutes, which further increased later. This difference could be due to the following reasons.

- The joist thickness in Test B1 was 1.15 mm and the joist thickness in Test 1 is 1.6 mm.
- In Test B1, plywood was used on the ambient side while in Test 1 plasterboards were used. Therefore after 80 minutes once the dehydration process of Pb2 finished, dehydration process of Pb3 started in Test 1, limiting the temperature rise on steel surfaces. But in Test B1, the steel surface temperature continued to increase along with plasterboard and plywood surfaces.
- Test B1 was conducted four years ago. The plasterboard quality could have been improved.
- The plasterboard joint in Test B1 could have been a weak joint and the measurements of hot flange surface temperatures could have been undertaken very close to the joint. In Test 1, the horizontal plasterboard joint could have lasted longer than in Test B1.
- In Test 1, channel sections were used as lateral restraints to floor joists at 600 mm intervals. Therefore the OHF surfaces temperature would have been transferred to the ambient side by conduction through larger steel area.

In Fig. 20 (b), the comparison of Tests 3 and B2 shows a similar behaviour to the comparison of Tests 1 and B1. But in both comparisons, the OHF temperature profiles from this study are lower than those from Baleshan and Mahendran's (2010) study. The use of steel channel sections with high conductivity in Tests 1 and 3 meant that heat would have been absorbed by them that led to the above variations in OHF temperatures.

In Baleshan and Mahendran's (2010) study, Tests B1 and B2 were conducted for floor specimens made of lipped channel sections and a LR of 0.4. But in this study, Tests 1 and 3 were conducted for floor specimens made of a hollow flange section and a LR of 0.2. The average failure HF temperatures of Tests B1 and B2 were 489°C and 504°C, respectively. But they were 712°C and 901°C for Tests 1 and 3, respectively. In the current study, hollow flange sections (LSBs) made of Duograde steel were used as floor joists. These LSB sections have a different

manufacturing process. Therefore, their elevated temperature mechanical properties could be considerably different. The difference in failure temperatures could have been caused by this.

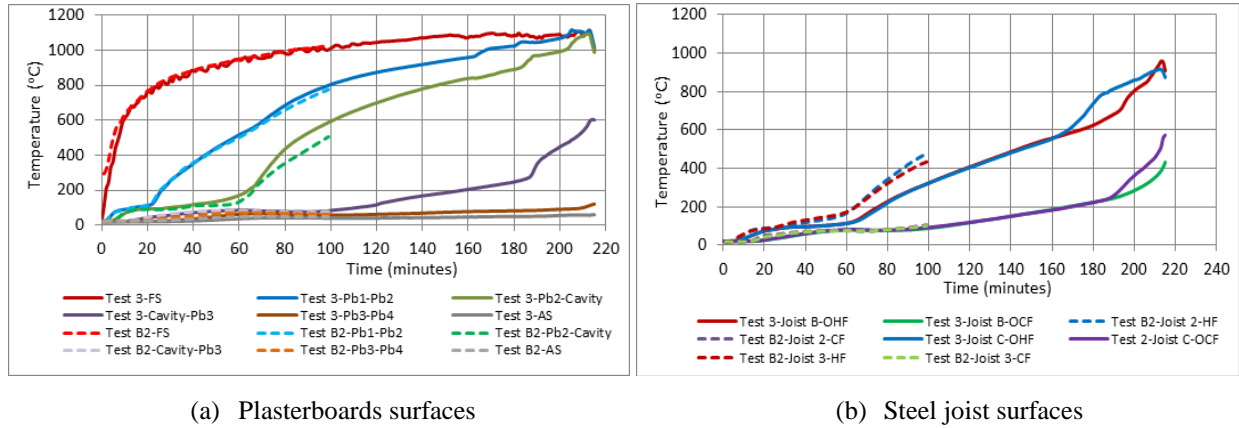


Figure 20: Average time-temperature profiles compared between Tests 3 and B2

Higher failure times of Tests 1 and 3 show the superior fire performance of these LSF floor systems made of LSB joists. This superior fire performance may be due to the different shape of the joist section. The better connectivity between the plasterboards and steel joists may also have contributed to this. Due to the presence of inner and outer flanges in LSB sections, the connectivity between plasterboards and joists could have lasted longer during fire tests.

5. Comparison of floor joist capacities from tests with predictions from fire design rules

5.1 Mechanical properties at elevated temperatures

The mechanical properties of LSB sections could be quite different due to their unique manufacturing process. Therefore their mechanical properties were determined using tensile tests of coupons taken from the web, inner flange and outer flange elements. Table 4 shows the average mechanical property results from these tests while Fig. 21 shows the stress-strain curves. The mechanical properties at elevated temperatures were then determined based on the reduction factors provided in Eurocode 3 Part 1.2 (ECS 2006) and are given in Table 5.

Specimen	Elastic Modulus (MPa)	Yield Strength (MPa)	Ultimate Strength (MPa)
Web	196100	464	558
Outer Flange	198717	602	656
Inner Flange	189786	520	574

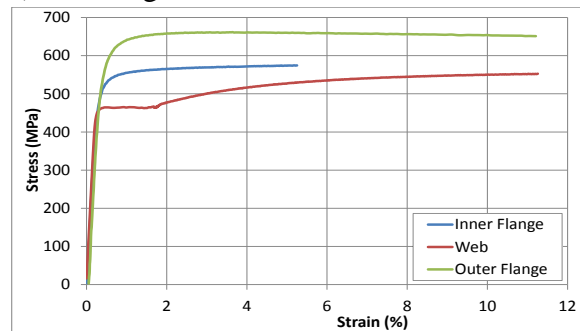


Figure 21: Stress-strain curves from tensile tests

5.2 Comparison of section moment capacities based on cold-formed steel design standards

Eurocode 3 Part 1.3 (ECS 2006) and AS/NZS 4600 (SA 2005) provide suitable design rules for cold-formed steel members. But they only provide them at ambient temperature. Based on these ambient temperature design rules, Baleshan (2011) proposed two simple design rules to predict

the moment capacity of cold-formed steel joists under fire conditions. He used the average joist temperature as the critical failure temperature in his proposed methods.

Table 5: Elevated temperature mechanical properties of LSB based on Eurocode 3 Part 1.2 (ECS 2006)

Temperature (°C)	Reduction factor of E	Reduced Elastic Modulus (MPa)	Reduction factor of f_y	Reduced Yield Strength (MPa)
20	1.00	200000	1.00	602.00
100	1.00	200000	1.00	602.00
200	0.90	180000	0.89	535.78
300	0.80	160000	0.78	469.56
400	0.70	140000	0.65	391.30
500	0.60	120000	0.53	319.06
600	0.31	62000	0.30	180.60
700	0.13	26000	0.13	78.26
800	0.09	18000	0.07	42.14
900	0.0675	13500	0.05	30.10

5.2.1 Method 1

The section moment capacities of LSF floor joists subjected to non-uniform temperature distributions were determined using Eq.1 based on AS/NZS 4600 (SA 2005). This method included the effects of elevated temperatures on the effective cross-section calculations of joists. The effective centroid was calculated based on the calculated effective widths. However, only the average elevated temperature was considered with a uniform temperature distribution across the joist.

$$M_{x,eff} = Z_{eff,T} f_{y,T} \quad (1)$$

where $Z_{eff,T}$ is the effective section modulus calculated based on the effective element widths at elevated temperature T, $f_{y,T}$ is the yield stress at the average joist temperature T (web).

Table 6: Elevated temperature mechanical properties of joists based on failure joist temperatures

Tests	Outer Hot Flange Temperature (°C)	Outer Cold Flange Temperature (°C)	Average Joist Temperature (°C)	Reduced Elastic Modulus E_T (MPa)	Reduced Yield Strength $f_{y,T}$ (MPa)
Test 1	712	601	656.5	41660	122.78
Test 2	715	595	655	42200	124.31
Test 3	901	573	737	23040	64.89
Test 4	620 ¹	510 ¹	565	82300	229.06

1-These temperatures are assumed based on the time-temperature profiles of Test 1

Table 7: Comparison of section moment capacities based on Method 1 with fire test results

Tests	Failure Joist Temperature (°C)	E_T (MPa)	$f_{y,T}$ (MPa)	$Z_{eff,T}$ (10^3mm^3)	$M_{x,eff}$ (kNm)	Failure Moment in Tests (M_s) (kNm)
Test 1	656.5	41660	122.78	37.860	4.65	4.62
Test 2	655	42200	124.31	37.867	4.71	4.62
Test 3	737	23040	64.89	38.428	2.49	4.62
Test 4	565	82300	229.06	38.579	8.84	9.24

Table 6 presents the average joist failure temperatures of the fire tests and the respective elastic modulus and yield strength values of steel at the failure temperatures. The failure temperatures of OHF and OCF surfaces of the joist in Test 4 were assumed based on the time-temperature profiles obtained in Test 1 since the time-temperature profiles of Tests 1 and 4 were almost similar. Table 7 compares the section moment capacities of floor joists at elevated temperatures calculated using Eq.1 and the failure moments for all the four tests. There is a very good agreement except for Test 3. In Test 3, after about 180 minutes the OHF surface temperature started to increase rapidly and reached 901°C due to the fall off of fire side plasterboards. In addition, excessive deflection caused by the higher temperature difference across the joist would have created a gap between the cavity insulation that would have eventually increased the OCF temperature. This could have then reduced the section moment capacity of floor joist in Test 3.

5.2.2 Method 2

This method does not include the effect of elevated temperatures on the effective width calculations. It was directly included in the form of reduction factors at the respective average joist temperatures. The section moment capacity of LSF floor joist is predicted using Eq.2.

$$M_{x,eff} = (k_{E,T}/k_{y,T})^{0.5} Z_{eff,20} f_{y,T} \quad (2)$$

where $Z_{eff,20}$ is the effective section modulus at ambient temperature, $k_{y,T}$ is the yield strength reduction factor at temperature T_{web} reached at time t , $k_{E,T}$ is the elastic modulus reduction factor at temperature T_{web} reached at time t , $f_{y,T}$ is the yield stress at the average joist temperature T (web).

Table 8: Comparison of section moment capacities based on Method 2 with fire test results

Tests	Failure Joist Temperature (°C)	Reduction factor of E $k_{E,T}$	Reduction factor of f_y $k_{y,T}$	$(k_{E,T}/k_{y,T})^{0.5}$	$Z_{eff,20}$ (10^3mm^3)	$M_{x,eff}$ (kNm)	Failure Moment in Tests (M_s) (kNm)
Test 1	656.5	0.2083	0.2040	1.0106	37.600	4.67	4.62
Test 2	655	0.2110	0.2065	1.0108	37.600	4.72	4.62
Test 3	737	0.1152	0.1078	1.0338	37.600	2.52	4.62
Test 4	565	0.4115	0.3805	1.0399	37.600	8.96	9.24

Table 8 shows the comparison of calculated section moment capacities of floor joists at elevated temperatures based on Eq. 2 and failure moments in all four tests. There is a very good agreement except for Test 3. The reason for this difference is similar to that discussed for Method 1. Therefore it is concluded that the proposed design rules of Baleshan (2011) based on the critical average joist temperature predicts the section moment capacities of LSF floor joists under fire conditions reasonably well. But they do not include the non-uniform temperature distribution across the joists, and therefore the accuracy of these methods is questionable.

6. Conclusions

This paper has presented the details of full scale fire tests conducted for LSF floors made of hollow flange joist sections and the comparisons of test results with predictions from available fire design rules. Test results showed that cavity insulation adversely affected the structural and fire performances of floor specimens due to excessive deflection caused by higher thermal bowing effects. The presence of plasterboard joints and plasterboard fall-off were found to have

a significant effect on the temperature development of steel surfaces and the failure times of LSF floors. The comparison of results from this research and Baleshan and Mahendran (2010) has shown that floor systems made of hollow flange joist sections have superior fire and structural performances over those made of lipped channel sections. Furthermore, the reduction factors of the elevated mechanical properties of these joist sections will have a major role on the fire performance of floor systems. Section moment capacities predicted based on Baleshan's (2011) design rules agreed well with the failure moments from the full scale fire tests. However, the effect of non-linear temperature distribution across the floor joists should be addressed.

In conclusion, this research has shown that the fire resistance ratings of LSF floors made of hollow flange sections showed a significant improvement over the conventional floor systems. This could be due to many reasons such as improved quality of plasterboard, joist section profile and elevated temperature mechanical properties of steel used. However, detailed numerical analyses along with the measured mechanical properties at elevated temperatures are required to fully understand the behaviour of these improved floor systems.

Acknowledgments

The authors would like to thank Australian Research Council for their financial support and the Queensland University of Technology for providing the necessary facilities and support to conduct this research project.

References

- Alfawakhiri, F. (2001). "Behaviour of cold-formed steel framed walls and floors in standard fire resistance tests." *PhD Thesis*, Carleton University, Ottawa, Ontario, Canada.
- Anapayan, T., Mahendran, M., Mahaarachchi, D. (2011). "Section moment capacity tests of LiteSteel beams." *Thin-Walled Structures*, 49 (1) 502-512.
- Baleshan, B., Mahendran, M (2010). "Improvements to the fire performance of light gauge steel floor systems." *Proc. of the 20th International Specialty Conference on Cold-formed Steel Structures*, Missouri, USA.137-154.
- Baleshan, B. (2011). "Numerical and experimental studies of cold-formed steel floor systems under standard fire conditions." *PhD Thesis*, Queensland University of Technology, Brisbane, Australia.
- EN 1993-1-2. (2005). "Eurocode 3: Design of steel structures. Part 1-2: General rules-Structural fire design." *European Committee for Standardization*, Brussels.
- EN 1993-1-3. (2006). "Eurocode 3: Design of steel structures. Part 1-3: General rules-Supplementary rules for cold-formed members and sheeting." *European Committee for Standardization*, Brussels.
- Kaitila, O. (2002). "Finite element modelling of cold-formed steel members at high temperatures." *Licentiate Thesis*, Helsinki University of Technology Laboratory of Steel Structures, Espoo.
- Sakumoto, Y., Hirakawa, T., Masuda, H., Nakamura, K. (2003). "Fire resistance of walls and floors using light-gauge steel shapes." *Journal of Structural Engineering*, 129 (11) 1522-1530.
- Standards Australia (SA). (1997). "AS/NZS 2589.1: Gypsum linings in residential and light commercial construction—application and finishing. Part 1: Gypsum plasterboard." Sydney, Australia.
- Standards Australia (SA). (1998). "AS/NZS 2588: Gypsum plasterboards." Sydney, Australia.
- Standards Australia (SA). (2005). "AS 1391: Methods for tensile testing of metals." Sydney, Australia.
- Standards Australia (SA). (2005). "AS 1530.4: Methods for fire tests on building materials, components and structures. Part 4: Fire resistance tests of elements of building construction." Sydney, Australia.
- Standards Australia (SA). (2005). "AS/NZS 4600: Cold-formed steel structures." Sydney, Australia.
- Sultan, M.A., Seguin, Y.P., Leroux, P. (1998), "Results of fire tests on full-scale floor assemblies." *Internal Report*, National Research Council of Canada, Ottawa, Ontario, Canada.
- Zhao, B., Kruppa, J., Renaud, C., O'Connor, M., Mecozzi, E., Azpiazu, W., Demarco, T., Karlstrom, P., Jumppanen, U., Kaitila, O., Oksanen, T., Salmi, P. (2005), "Calculation rules of lightweight steel sections in fire situations." *Research Report*, Technical Steel Research, European Union.